Characterization of Soil and Rock Hosting an Aquifer in Southeast Panama City using Geotechnical, Geophysical and Geochemical Parameters

Ana Cristina González Valoys (ana.gonzalez1@utp.ac.pa)
Universidad Tecnologica de Panama https://orcid.org/0000-0001-5963-2289
Miguel Vargas-Lombardo
Universidad Tecnológica de Panamá: Universidad Tecnologica de Panama
Raimundo Jimenez-Ballesta
Universidad Autonoma de Madrid - Campus de Cantoblanco: Universidad Autonoma de Madrid
Jonatha Arrocha
Universidad Tecnológica de Panamá: Universidad Tecnologica de Panama
Eric Gutiérrez
Universidad Tecnológica de Panamá: Universidad Tecnologica de Panama
Efrén García-Ordiales
Universidad de Oviedo
Pablo Cienfuegos
Universidad de Oviedo
Francisco García-Navarro
Universidad de Castilla-La Mancha
Pablo Higueras
Universidad de Castilla-La Mancha

Research Article

Keywords: aquifer, geotechnical, geophysical, geochemistry, marlstone

Posted Date: June 15th, 2021

DOI: https://doi.org/10.21203/rs.3.rs-583654/v1

Abstract

The aim of the present study is to assess the combined use of geotechnical and electrical geophysical methods to determine water quality and rocks mechanics in an aquifer. The aquifer studied is located in the Tocumen sector of Panamá City, located to the southeast of city, where there is a need to study the possible use of this aquifer to provide drinking and/or irrigation water based on its quality. To this end, a 10 m well was perforated and sampled to characterize the host soil and rock trough granulometry, determine the Atterberg limits, measure the physicochemical parameters and perform a chemical analysis, including reactivity (pH), electrical conductivity (EC), organic matter content, cation exchange capacity, calcium carbonate, sulfates, chlorides, SiO_2, Al_2O_3, Fe_2O_3, CaO, MgO, SO_3, Na_2O and K_2O. In addition, a 2D electrical resistivity tomography profile was conducted in order to correlate the electric parameters with the physicochemical and chemical ones and extend them laterally to check the continuity of the characteristics measured. The results show a good correlation between geotechnical, geophysical and chemical parameters, thus highlighting the presence of discontinuities that must be overcome by infiltrated rainwater to reach the deepest levels, which are characterized by the presence of water. The water chemistry varies with depth, with sodium bicarbonated water being the predominant facies.

1. Introduction

Water is a prime resource needed for human consumption, agriculture, livestock and industry that is in increasingly short supply. Tropical countries with high to very high pluviosity have traditionally experienced few problems in terms of water supply, although two aspects typically affect this situation: the irregular distribution of rain, with heavy storm episodes that are difficult control in terms of water storage, and the need for appropriate infrastructures to collect and store the corresponding huge quantities of water deposited during such events, which are also often lacking in these countries. This is the case for Panamá City, the capital of the Republic of Panamá. This city, which supports a population of 880,691 (Contraloría General de la República de Panamá 2010), is located on the Pacific Ocean coast. Under the Köppen climate classification, Panama City has a tropical savanna climate (Köppen Aw), which is a little drier than a tropical monsoon climate. It typically sees 1900 mm (74.8 in) of precipitation annually. The wet season spans from May through December, and the dry season spans from January through April (Dirección de Meteorología de ETESA 2007). Temperatures remain constant throughout the year, averaging around 27°C (81°F) (Servicio de Información Meteorológica Mundial, 2008). Furthermore, flooding events, such as those which occurred in December 2010 (the so called “Storm of the Purisima”), which led to torrential rains that increased the turbidity of reservoir lakes and disabled the production of drinking water at the water treatment plant, sometimes occur in this region. It took almost three months to resolve this problem, thus leaving Panama City without this vital liquid (La Estrella de Panama 2012). In light of this, ground water could be an appropriate alternative to the water supply during such catastrophic events or during eventual drought periods.

The present study is intended to gain a better understand of the nature of the groundwater stored in the Tocumen sector, located to the ENE of the town center (González-Valoys et al. 2021). We have extended research to a study of the host soil and rocks, in order to understand the relationship between water and its hosts, based on the geophysical properties (electric resistivity) of the site, the geotechnical parameters of the soil and rock, the physicochemical and geochemical parameters of the soil and rock, and the chemical composition of the water contained therein (De Caro et al. 2017; Shomar 2015). This synergic combination of techniques was expected to provide sound and reliable information to assess the possibilities of this aquifer to be used as a reliable water supply (Abdel-Satar et al. 2017; Armengol et al. 2017; Chidya et al. 2015; Zhang et al. 2018). The area studied is located close to both the urban area and the Pacific coast, where human and industrial activities that may have negative impacts on the aquifer are conducted (Appelo & Postma 2004; Bakhshipour et al. 2016; Jordanova et al. 2013).

The methodology applied in the present study is based on several complementary techniques: a 10 m deep well was drilled in the area, thus allowing us to sample and characterize the soil and rock using physicochemical and geotechnical parameters, as well as chemical analysis. In addition, geophysics, using 2D electrical resistivity tomography (ERT) (Mojica et al. 2013; Ho et al. 2017; Benabdelouahab et al. 2018) provided a basic scenario of lithologies in the area and alloweds a lateral interpretative extension of data provided by the section obtained in the well.

2. Materials And Methods

2.1 Study area

The study site is located at latitude coordinates 9°3’57.93” N and longitude 79° 24’23.22” W, in the southeast coastal area of the Isthmus of Panama. The Tocumen sector of Ciudad de Panamá, which corresponds to an industrial and residential sector in which part of the Technological University of Panamá is located, constitutes the ENE outskirts of the city. Its topography is almost plain, with marshes and mangroves extending from the site to the coast (~ 5000 m.).

It has characteristic tropical climate (Awi type, savanna tropical climate) according to the Köppen climate classification map, with annual rainfall > 1000 mm (Dirección de Meteorología de ETESA 2007). Figure 1 shows the climograph with data from the ETESA meteorological station from 2012 to 2020 (Dirección de Meteorología de ETESA 2021), from which it can be seen that the dry season includes the months of January to March (lowest rainfall) and the rainy season from April to December, the rainiest months being October and November. As for the temperature, the highest temperatures are found in the dry months.

The lithology of the area includes marine sedimentary rocks belonging to the Panamá Formation, from the Tertiary age (Fig. 2). It consists mainly of tuffaceous sandstones, tuffaceous shales and limestones (Guardia 2018). Petrographic analysis of the rock in this area shows that it comprises marly siltstone (marl), with a clastic structure and uniform texture, formed from silt-size fragments of micrite, shells and

fragments of microfossils (microforaminifers), with abundant chloritic-clayey material, sporadic fragments of silicates (includes quartz and especially feldspars, rare Fe-Mg minerals), some traces of carbonous material, and very rare magnetite (Gutiérrez 2021).

A water well with a depth of 24 m that is used sporadically for water production, with a small pump of 1.5 Hp, has been installed at the site since 1993 (Vega 2004). In a preliminary test, it was determined that with a pumping flow of 2.52 L/s, the efficiency of the well (UTP-ET) was 87.9%. The Cooper & Jacob Method (Kruseman et al. 1970) gave a preliminary transmissivity (T) value of 21.1 m^2/day, and a storage coefficient (S) of 2.08 x 10^{-3} was obtained using the Theis Method (Kruseman et al. 1970). Given this value of S, the aquifer is semi-confined and presents a vertical percolation according to the Abatement *vs.* Time curve (Vega 2004). In a pumping test at constant flow for 72 hours carried out in October 2015, it was determined that100% efficiency is obtained with a flow of 1.26 L/s, and the well stabilizes at 6.15 meters (Alpirez et al. 2015). The hydraulic gradient is relatively low, with a value of 6.10 x 10^{-4}. Given that the area is flat and with little slope, the flow direction goes from south to north (Alpirez et al. 2015).

The recharge of an aquifer is very important (Abiye et al. 2018; Barbera et al. 2018; Healy & Cook 2002; Martínez et al. 2017), and Fig. 3 shows the graph of the temporal evolution of the water table in the studied well (Centro de Investigaciones Hidráulicas e Hidrotécnicas 2016) *vs.* rainfall (Dirección de Meteorología de ETESA 2021) for the year 2014, which shows that the rainfall in the area directly influences the water table in the well since, in the dry months, in the absence of rain, the water level decreases. The much higher rainfall during the rainy season rapidly produces a net recharge of the water level in the well.

2.2 Analytical work

Field and laboratory studies were carried out between June and August 2015 at the Experimental Engineering Center (CEI), Technological University of Panamá.

The Geotechnical Laboratory (LABGEO), Technological University of Panamá, drilled a well 10 meters deep, with a diameter of 75.7 mm, in the area adjacent to the well where the hydrogeochemical study was carried out (Fig. 4a). Drilling was performed using a rotary diamond drilling machine (Acker, model AD-II) with a double-tube recovery system. The water table was detected at a depth of 2.50 m 24 hours after completion of the drilling (Arrocha 2015). During drilling, the Rock Quality Designation (RQD) parameter was estimated. This parameter indicates the degree of jointing or fracture in a rock mass measured in percentage, where an RQD of 75% or more shows good quality hard rock and less than 50% show low quality weathered rock (The Constructor 2018).

In parallel, the Engineering and Applied Sciences Research Laboratory (LIICA), Technological University of Panamá, performed a 2D electrical resistivity tomography, over a length of 40 meters. This was carried out using a Syscal R1 resistivity meter (http://www.iris-instruments.com/syscal-r1plus.html), with a multicable system, powered by a 12V battery; 41 electrodes were used, with a separation of 1 meter, the Wenner-Schlumberger configuration of which allowed us to obtain good resolution tomography to a

depth of 8 meters. Data were processed using the Earthlmanger 2D software (https://www.agiusa.com/agi-earthimager-2d) and exported to Surfer 12 (https://www.goldensoftware.com/products/surfer) for representation (Mojica 2015).

Four samples, corresponding to the different lithologies observed in the drill's profile, were taken (Table 1; Fig. 4). Samples corresponding to complete soil and to fragments of the underlying rock were taken using gloves, stored in plastic bags and kept at room temperature until analysis.

Sample preparation included sieving of the soil sample to separate the > 2 mm fraction. Rock fragments were crushed and then also sieved to < 2 mm. Additionally, samples for geochemical analyses were prepared by CEMEX, including grinding to < 100 µm.

Table 1
Identification of samples

Identification	Depth	Visual description
Sample 1	0.00–0.10 m	Topsoil
Sample 2	0.10–1.00 m	Brown rock
Sample 3	1.00–2.90 m	Light brown rock
Sample 4	2.90–10.00 m	Light grey rock

Physicochemical parameters were determined by the Industrial Analysis and Environmental Sciences Laboratory (LABAICA). The methodologies applied included ASTM D 4972 (for pH and EC) in a 1:5 suspension (w/V) using a multi-parameter benchtop Orion Versa Star Pro device; ASTM D 2974 for organic matter content, by weight loss at 455°C; cationic exchange capacity (CEC) using the potentiometry method (Weaver et al. 1991); calcium carbonate determination according to Skinner & Halstead (1958); sulfate determination based on ASTM D1580 (ASTM 2004); and chloride determination as per AASTHO T-291 (2013). Geochemical analyses included SiO_2, Al_2O_3, Fe_2O_3, CaO, MgO, SO_3, Na_2O and K_2O, and was carried by CEMEX Panama using the X-ray fluorescence technique.

The non-organic soil (Sample-2) was also characterized by determining the Atterberg limit (ASTM D4318), and the granulometry (ASTM C6913) by texture classification according to the Unified Soil Classification System (USCS) (ASTM D 2487) (ASTM 2004).

The mechanical behavior of unweathered rock (three subsamples of Sample 4) was established by axial compression testing (ASTM D 7012) (ASTM 2004) using an ELE International device (model ACCU-TEK 350 digital series).

3. Results

3.1 Geotechnical Tests

Geotechnical parameters (Table 2) indicate that the soil (Sample-2) corresponds to the GC group (clay gravel with sand), according to the results obtained from the grain size and the Atterberg limits for the USCS (Unified Soil Classification System).

Table 2
Classification (granulometric analysis and consistency limits)

Hole	Sample-2
Sampling depth (m)	0.10–1.00
USCS classification	GC
Description	Clay gravel with sand
Color	Light brown
Liquid Limit, LL	61
Plastic limit, PL	26
Plasticity index, PI	35

The results of axial compression test applied to three subsamples of sample 4 (4 − 1, 4 − 2 and 4 − 3) are shown in Table 3. These values can be considered as normal for lutitic rocks (Kiamco et al. 2004). In addition, the results of the visual inspection of discontinuities seen in the rock in the interval 2.9 to 10 m (samples 3 and 4) are presented in Table 4.

Table 3
Axial compression to rock cores

Hole	Sample	Depth (m)	q_u (kg/cm^2)	γ_m (kg/m^3)	v_s (m/s)	E_{av} (kg/cm^2)
H-1	sample 4 − 1	6.40	151	2064	618	19 266
	sample 4 − 2	7.60	161	2175	869	40 179
	Sample 4 − 3	9.80	185	2149	899	42 478

Table 4
Description of discontinuities.

1. Discontinuity spacing	**Description**	**Spacing**	**Designation of rock mass**
	Spaced to widely spaced	**0.60 to 2.00 m**	**Massive to solid**
2. Condition of discontinuities	**Roughness**	**Opening**	**Filling thickness**
	Wavy smooth	Moderately open to closed	Very thin film
3. Designation of rock quality	From regular to excellent		
4. Persistence of discontinuities	Cannot be defined		
5. Orientation	The joints dive at different angles		
6. Presence of water in discontinuities	The fracture is dry but shows evidence of flow circulation, such as stains and leaching.		

3.2 Electrical Resistivity Tomography

This technique is widely used in hydrogeological studies as it allows an estimation of the presence of groundwater as well as an interpretation of the stratigraphy of the site, without the need for drilling. The electronic configuration used corresponds to an arrangement of the Wenner-Schlumberger type, which allows the structure to be visualized laterally and in depth, with good resolution and depth for research in the study area. The 2D electrical resistivity tomography had 19 levels of depth and 380 values of apparent resistivity, thus providing a distribution section of the measured data. This representation does not quantify the actual distribution of the data as it is the result of the inversion that gives a distribution of the electrical resistivity of the subsoil at an actual depth (Mojica 2015).

3.3 Soil and Rock Physicochemical Tests

Table 5 shows the results obtained in the different physicochemical tests for soil and rock found at the site. The reactivity (pH) ranges from 8.21 in the topsoil to 7.61 in the marlstone. Following the same trend with depth, the percentage organic matter content decreases from 5.99 to 1.62; SiO_2 from 59.22 to 54.70; Al_2O_3 also decreases from 13.19 to 10.03; and Fe_2O_3 from 6.63 to 4.57. On the other hand, the EC increases strongly with depth (from 0.258 to 2.220 dS/cm), thus suggesting an increase in salinity. $CaCO_3$ also increases (from 5.12 to 19.12%), as do CEC (from 24.32 to 46.17 meq/100 g), the CaO content (from 1.81 to 4.03), MgO (from 2.02 to 2.48) and Na_2O (from 1.44 to 2.37).

Table 5
Physicochemical parameters and geochemical analysis for soil and rock.

Parameters	Sample 1	Sample 2	Sample 3	Sample 4
pH	8.21	8.39	8.82	7.61
Electric conductivity (dS/cm)	0.258	0.312	0.250	2.220
Organic matter content (%)	5.99	5.68	4.14	1.62
Calcium carbonate (%)	5.12	6.11	11.84	19.12
Sulfates (mg/kg)	< 0.02	<0.02	<0.02	0.28
Chlorides (mg/kg)	< 1.0	22.1	11.0	< 1.0
Cation Exchange Capacity (meq/100 g)	24.32	27.90	40.65	46.17
SiO_2 (%)	59.22	58.88	57.41	54.70
Al_2O_3 (%)	13.19	12.49	11.18	10.03
Fe_2O_3 (%)	6.63	5.84	4.24	4.57
CaO (%)	1.81	2.47	3.50	4.03
MgO (%)	2.02	2.01	1.75	2.48
SO_3 (%)	0.07	0.09	0.08	4.90
Na_2O (%)	1.44	1.41	1.44	2.37
K_2O (%)	0.87	0.84	0.93	0.77

4. Discussion

On the basis of the results obtained for the physicochemical and geotechnical parameters, the profile studied, as expressed in Table 6, corresponds to a relatively soft and fractured sedimentary, overlayed by a residual soil, with a lower than expected thickness for this region. In particular, the soil extends to a depth of 1 meter and consist of a very thin “A” type horizon, which very rich in organic matter, whereas the rest of the soil corresponds to a “C” type horizon, with important presence of a gravel fraction. This AC soil is not at all characteristic of soils from areas characterized by a savanna tropical climate, in which the rainy weather promotes much more complete profiles. On this basis, the soil can be interpreted as a technosol or anthrosol, possibly corresponding to a more complete soil partly dismantled by human activities in a residential/industrial area. The area corresponds to a type C soil profile, which is a dense soil and soft rock, since its cut-off velocity value (vs) is 694 m/s.

Table 6
Stratigraphy of the profile.

Depth	Stratigraphy
Sample 1	Organic layer, including vegetation waste.
Sample 2	Soil, constituted by clayey gravel with sand.
Sample 3	Sedimentary, weathered rock, very poor quality, light brown color.
Sample 4	Sedimentary rock, with, moderately soft hardness (RH-2), weak resistance, quality of regular to excellent, light gray color.

The rest of the profile (1–10 m. depth) corresponds to a solid rock, constituted by marlstones, with sedimentary lamination. It is possible to distinguish between the depth from 1 to 2.9 m, which corresponds to partly weathered rock, as evidenced by its light brown color (evidence of preliminary formation of Fe oxyhydroxides), and the rest of the profile (2.9 to 10 m deep), where the rock appears to be unweathered, with the original greyish color. The discontinuities in both the weathered rock and healthy sedimentary rock (marlstone; see Table 4) suggest the circulation of water through them, which indicates that there is infiltration of rainwater through the rocks, thus allowing the aquifer to be replenished (Arrocha 2015; Medici et al. 2016). The values for the axial compression not confined to rock cores in sub-samples 4 were similar to those reported in marl rocks from Saudi Arabia and Jordan (Shaquor et al. 2008; Mustafa et al. 2017)

Figure 5 shows the drilling profile at a depth of 10 meters, with indications of the parameters estimated by visual inspection. In particular, the RQD values, together with observational data for fracturation-related discontinuities (Table 4), are an indication of a healthy rock with a very low degree of tectonic fracturation. In addition, the discontinuities in the rock show evidence of water flow which, together with the lack of evident intergranular porosity and permeability, suggests that the aquifer is hosted in a fractured rock (Healy & Cook 2002). Moreover, the pumping test suggested that it is a semi-confined aquifer, as shown in the previous report by Vega (2004).

The 2D tomography survey corroborated the presence of groundwater, coinciding with the limit between the weathered and unweathered rock (Mojica et al. 2012; Mojica 2018), as shown in Figs. 6 and 7.

The smooth inversion method (see Fig. 6) included three interactions and an RMS calculation error of 2.58%. The robust inversion method (Fig. 7) also included three interactions and an RMS calculation error of 2.83% (Mojica, 2015). Although the error in the robust inversion is slightly larger than that for the soft one, both figures basically show the same calculated electrical resistivity profile for the terrain. Both figures show the inversion profile compared to the drilling profile. The calculated electrical resistivity tomographs correspond very well with the mechanical drilling profile of the terrain. The surface layer, corresponding to the topsoil and soil, is shown in green and presents intermediate resistivity values. The resistivity areas (expressed in the profile in blue) seen in this layer indicate the presence of moisture on

the ground surface, since tomography was performed in the rainy season. The high resistivity layer (in yellow and red colors) identified at greater depths should represent healthy sedimentary rock. Finally, at the bottom, an additional low resistivity (blue) area, which indicates a high moisture content, that is, the presence of groundwater in the aquifer, is observed.

The interpretation of the electrical tomography profile allows us to deduce an irregular topography in the contact between the soil and the rock substrate (Fig. 8). This topography, formed by grooves and peaks, is probably related to the fracturing observed in the test core. This character also allows us to differentiate two types of aquifers, both of which are fractured. The upper aquifer, hosted in the soil, corresponds to a free aquifer concentrated in areas of strongly fractured rocks and which, in turn, is delimited by some type of impermeable fracture. The lower aquifer corresponds to a semi-confined aquifer, presents less fracturing and is delimited by fractures such as those observed; it is presumed to be in contact with the upper aquifer via some of these fractures.

Figure 9 shows an attempt to correlate the results obtained for the geotechnical profile, the 2D electrical resistivity tomography and the geochemistry results. This figure presents the drilling profile at 10 meters, together with the variations in the calculated electrical resistivity and some geochemical parameters such as CIC, % $CaCO_3$, pH and % organic content. As can be seen, the calculated electrical resistivity of the subsoil decreases in the layer of clayey gravel and sedimentary rock to the water table (1.5 m), then increases at a depth of 4 m before decreasing again at a depth of 8 m.

As for the physicochemical tests of soil and rock, we observed that the reactivity (pH) ranges between 7.4 and 8.5 in the different layers, corresponding to moderately alkaline soils (Weaver et al. 1991). Thus, the organic layer, the clay gravel and the healthy sedimentary rock showed moderately alkaline pH, whereas the weathered sedimentary rock showed a strongly alkaline pH of more than 8.5.

According to the classification table for the EC in soils proposed by Vázquez and Bautista (1993), an EC of 0–2.0 dS/m corresponds to non-saline soils and 2.1–4.0 dS/cm to low salinity soils. As such, the organic layer, soil and weathered rock (0.250 to 0.312 dS/m) correspond to a non-saline terrain, whereas the healthy sedimentary rock, with an EC of 2.22 dS/m, should have an even lower salt content.

The organic matter content is, as expected, higher in the thin topsoil layer (5.99%) and decreases with depth, having a value of 5.68% in the “C” horizon, and much lower in the rock (4.14% in the weathered sedimentary rock, possibly indicating some infiltration of colloidal organic matter from the overlying soil, and 1.62% in the healthy sedimentary rock).

The values obtained for the $CaCO_3$ content increase with depth, with values of 5.12% for the organic layer, 11.84 % for weathered rock and 19.12% for healthy sedimentary rock. This value implies that this host rock is a calcareous marlstone. However, it is not easy to determine whether the lower $CaCO_3$ content for the weathered rock corresponds to an original difference in composition, possible in marlstone sequences (Derriche & Cheikh-Lounis 2004), or if this difference is a consequence of the higher degree of weathering of this level, which would imply the partial hydrolysis and washing of this component. In any case, the

chemistry of the local groundwater, which is of the sodium bicarbonate type, with HCO_3^- values in groundwater of between 215.40 and 278.85 mg/L (González-Valoys et al. 2021), is a clear indication of the contribution of this lithology to its composition, as indicated by other studies in waters obtained from marlstone (Wersin et al. 2016).

The first three layers have sulfate values below the detection limit (0.02 mg/kg) of the method used, with the last layer having a value of 0.28 mg/kg SO_4^{2-}. These are low values for this anion, which is typically low in a marlstone lithology (Derriche & Cheikh-Lounis 2004). As expected, in parallel to the sulfate values, the % SO_3 is very low in the three most superficial samples, and higher in the deepest one. The groundwater has sulfate values of between 64.85 and 127.30 mg/L (González-Valoys et al. 2021), thus suggesting dissolution of the sulfates contained in the marls, as evidenced by another study of waters obtained for this lithology (Wersin et al. 2016).

The chloride ion has the peculiarity of moving and dissolving in the soil profile according to runoff and precipitation (Custodio & Llamas 1976; Tan et al. 2017). The samples for this study were taken in the transition from the dry to the rainy season, after the first rains that mobilize the soluble salts to the second layer had fallen. The presence of this anion may be related to the influence of marine aerosols, which are deposited on the topsoil then filter down to, and are concentrated in, the “C” horizon, acting in this location as a proto-“B” horizon. Concentrations in the marlstone rock are lower than unity, thus indicating that this rock does not contain chloride salts (Derriche & Cheikh-Lounis 2004). The groundwater has chloride values of between 11.20 and 22.37 mg /L (González-Valoys et al. 2021). In this case, the marl rock does not provide chlorides, but allows chloride-containing water to infiltrate from the surface (Appelo & Postma 2004; Shomar 2015).

The cation-exchange capacity (CEC) is the ability of soil to retain and exchange different mineral elements. This parameters depends on the texture of the soil and the organic matter content (Weaver et al. 1991). The CEC values are 24.32 meq/100g for sample 1, 27.90 meq/100g for sample 2, 40.65 meq/100g for sample 3 and 46.17 meq/100g for sample 4, thus being higher in the rock. The interchangeable cations of the analyzed samples are likely to be K^+, Ca^{2+}, Fe^{2+}, Na^+ and Al^{3+} (Custodio & Llamas 1976). The increase in CEC with depth explains the corresponding increase in % CaO, % Na_2O and % MgO, which are the main cations in the groundwate analyzed r (González-Valoys et al. 2021; Armengol et al. 2017; Martinez et al. 2017). With respect to soil fertility, this parameter corresponds to a medium fertility soil (Vázquez & Bautista 1993), in case it is to be used for cultivation and planting purposes.

The concentration of other metal oxides, such as SiO_2, Al_2O_3 and Fe_2O_3, decreases as depth increases. Indeed, it can be seen that their values decrease with each layer. The K_2O content remains low in all layers since potassium is a minority cation in this type of sedimentary rock (Oke et al. 2017).

5. Conclusions

The profile studied corresponds to section including a portion of soil, around 1 m in depth, and a marl-type rock, the thickness of which is much greater than the depth drilled (10 m). The soil is probably a partial section of the original soil and is likely to have been partially excavated and dismantled for human-related activities.

According to the edaphological characterization, the residual soil studied corresponds to a technosol or anthrosol and can be considered to be a permeable and transmissive level that favors the infiltration of rainwater, as confirmed by the good correspondence between rainfall and water table rise. In addition, these characteristics also promote the infiltration of chlorides, which are present in the soils as a consequence of transportation in marine aerosols from the nearby ocean. However, the soil seems to be acting as a chemical barrier to this process by favoring the immobilization of this cation at this level.

The underlying sedimentary rock corresponds to a marl, in particular to a marly siltstone, with a $CaCO_3$ content of 19.12 %. It has a low but measurable content in sulfates, and a very low to null content in chlorides. Upon visual inspection, it is evident that in proximity to the soil-rock interface the rock is weathered, as indicated by a brownish color indicative of the incipient oxidation of Fe minerals present in the rock. As also evident in the visual inspection, and confirmed by the RQD determinations, the rock presents a certain degree of tectonic fracturation, which is likely to allow water to infiltrate and accumulate in the rock, thus constituting an aquifer.

The 2D electrical resistivity tomography confirmed the suitability of this technique for investigating the presence of water in the soil and subsoil. In particular, in this case the technique has also proven its ability to accurately identify the topography of the soil-rock interphase, and was also able to identify two water accumulations: one superficial, associated with the presence of water in the soil, and a deeper one, related to the fractured aquifer. Moreover, this technique correctly identified areas with higher fracturation ratios, which may be of interest for a detailed research of favorable sites for deeper drilling aimed at obtaining higher water reserve volumes.

There is a good agreement between the chemistry of the water, as characterized in a previous study, and that of the rock studied in the drill section, especially as regards the presence of carbonates and sulfates, alkaline pH, and medium to high cation-exchange capacity. These characteristics make the local water suitable for use in irrigation.

Based on our results, we recommend a more complete study of the possibilities of water production in this area, including a more extensive use of electrical tomography to find the most favorable areas, which will be characterized by higher tectonic fracturation. Other elements to bear in mind during that study should be to avoid proximity to the coast, to allow the infiltration of chlorides from marine aerosols to be minimized. The chemistry of the water should also studied further, including the characterization of possible pollutants related to human activities, given the proximity of the area to industrial and residential areas.

Declarations

Funding information:

This study was funded by the National Secretariat for Science and Technology (SENACYT) and the Institute for the Training and Use of Human Resources (IFARHU) of Panama (270-2019-109); and Fondos para Grupos de Investigación UCLM (2019-GRIN-27011).

Conflicts of Interest/Competing interest:

The authors declare no conflict of interest.

Availability of data and material:

Not applicable.

Code availability:

Not applicable.

Author Contributions:

The paper was written by Ana González Valoys, Miguel Vargas Lombardo, Eric Gutiérrez, Jonatha Arrocha, Efrén García Ordiales, Pablo Cienfuegos, Francisco Jesús García Navarro, Raimundo Jimenez Ballesta and Pablo Higueras. The physicochemical soils and rock samples were processed and analysed by Ana González Valoys, geotechnical tests were performed by Jonatha Arrocha and petrography by Eric Gutiérrez.

Animal research:

Not applicable.

Ethics approval:

Not applicable.

Consent to participate:

Not applicable.

Consent for publication:

Not applicable.

Acknowledgments:

The authors thank the Technological University of Panama for their collaboration during this research, the Center for Hydraulic Research and Hydrotechnical (CIHH), the Experimental Center of Engineering (CEI) and its laboratories, Laboratory of Geotechnics (LABGEO), Engineering and Applied Sciences Research Laboratory (LIICA), Industrial Analysis and Environmental Sciences Laboratory (LABAICA). We would also like to thank CEMEX Panama for collaborating with the X-ray fluorescence determinations, and the human team at each laboratory, especially David Vega, Dr. Alexis Mojica, Dr. Cecilio Hernández, Fidedigna de Ortiz, José Pérez and Ana Franco. The National Secretariat of Science and Technology (SENACYT) and Institute for the Training and Use of Human Resources (IFARHU) of Panama, and the University of Castilla-La Mancha (UCLM), University of Oviedo and the Autonoma University of Madrid (UAM), are also thanked for their support for this research. Thanks to Andrew Frankland (Scientific English) for the revision of the English style of the manuscript.

References

1. AASHTO T 291 (2013) Standard Method of Test for Determining Water-Soluble Chloride Ion Content in Soil, Single User Digital Publication. American Association of State Highway and Transportation Officials
2. Alpirez J, Aviles K, Chiari K, Chung Y, Pinzón I, Samudio M, Vega D (2015) Proyecto de Agua Subterránea, Acuífero de la UTP, Extensión Tocumen. pp 1–19
3. Abdel-Satar A, Al-Khabbas M, Alahmad W, Yousef W, Alsomadi R, Iqbal T (2017) Quality assessment of groundwater and agricultural soil in Hail region, Saudi Arabia. *The* Egyptian Journal of Aquatic Research (2017) 43, 55–64, http://dx.doi.org/10.1016/j.ejar.2016.12.004
4. Abiye T, Masindi K, Mengistu H, Demlie M (2018) Understanding the groundwater-level fluctuations for better management of groundwater resource: A case in the Johannesburg region. Groundwater for Sustainable Development 7:1–7. https://doi.org/10.1016/j.gsd.2018.02.004
5. Appelo C, Postma D (2004) Geochemistry, groundwater and pollution (CRC press) 2nd Edition, ISBN 0415364213, pp 1-649
6. Armengol S, Manzano M, Bea S, Martínez S (2017) Identifying and quantifying geochemical and mixing processes in the Matanza-Riachuelo Aquifer System, Argentina. Science of The Total Environment 599–600:1417–1432. https://doi.org/10.1016/j.scitotenv.2017.05.046

7. Arrocha J (2015) Informe sobre Ensayos Geotécnicos para el Estudio Hidrogeoquímico de las Aguas Subterráneas del Pozo Ubicado en la Extensión Tocumen, Universidad Tecnológica de Panamá; para la tesis de la Lic. Ana González (Panamá, Tocumen: Universidad Tecnológica de Panamá, Centro Experimental de Ingeniería, Laboratorio de Geotecnia), pp 1–24
8. ASTM (2004) Volume 04–09. In Annual Book of ASTM Standards. International Standard World Wide, American Society Testimg of Materials (ASTM). Section four, Constructions Volume 04.08 and 04.09, Soil and Rock (I). C6913, D1580. D2487, D2974, D4318, D4972, D7012
9. Bakhshipour Z, Asadi A, Huat B, Sridharan A, Kawasaki S (2016) Effect of acid rain on geotechnical properties of residual soils. Soils Found 56:1008–1020. https://doi.org/10.1016/j.sandf.2016.11.006
10. Barberá J, Jódar J, Custodio E, González-Ramón A, Jiménez-Gavilán P, Vadillo I, Pedrera A, Martos-Rosillo S (2018) Groundwater dynamics in a hydrologically-modified alpine watershed from an ancient managed recharge system (Sierra Nevada National Park, Southern Spain): Insights from hydrogeochemical and isotopic information. Sci Total Environ 640–641:874–893. https://doi.org/10.1016/j.scitotenv.2018.05.305
11. Benabdelouahab S, Salhi A, Himi M, Stitou El Messari J, Casas Ponsati A, Mesmoudi H, Benabdelfadel A (2018) Using resistivity methods to characterize the geometry and assess groundwater vulnerability of a Moroccan coastal aquifer. Groundwater for Sustainable Development 7:293–304. https://doi.org/10.1016/j.gsd.2018.07.004
12. Centro de Investigaciones Hidráulicas e Hidrotécnicas (2016) Data de niveles piezométricos del pozo de la Extensión Tocumen, Universidad Tecnológica de Panamá, pp 1–24
13. Chidya R, Matamula S, Nakoma O, Chawinga C (2015) Evaluation of groundwater quality in rural-areas of northern Malawi: Case of Zombwe Extension Planning Area in Mzimba. Phys Chem Earth 93:55–62. https://doi.org/10.1016/j.pce.2016.03.013
14. Contraloría General de la República de Panamá (2010) Retrieved 10th March 2021 from: http://www.contraloria.gob.pa/inec/archivos/P3551P3551cuadro3-08.xls
15. Custodio E, Llamas M (1976) Hidrología Subterránea. Ediciones Omega, Barcelona, Spain. Tomo I y II, ISBN 8428204462 obra completa, pp 1-2418
16. De Caro M, Crosta G, Frattini P (2017) Hydrogeochemical characterization and Natural Background Levels in urbanized areas: Milan Metropolitan area (Northern Italy). J Hydrol 547:455–473. https://doi.org/10.1016/j.jhydrol.2017.02.025
17. Derriche Z, Cheikh-Lounis G (2004) Geotechnical characteristics of the Plaisancian marls of Algiers. Bull Eng Geol Env 63:367–378. https://doi.org/10.1007/s10064-004-0246-5
18. Dirección de Hidrometeorología de ETESA (2007) Mapa de Clasificación Climática (según Köppen). Retrieved May 23, 2020 from http://www.hidromet.com.pa/mapas.php
19. Dirección de Hidrometeorología de ETESA (2021) ETESA Hidrometeorología, datos diarios. Retrieved March 21, 2021 from https://www.hidromet.com.pa/es/datos-diarios
20. González-Valoys A, Vargas-Lombardo M, Higueras P, García-Navarro F, García-Ordiales E, Jiménez-Ballesta R (2021) Hydrochemistry of groundwater from Tocumen sector, Panama city: an

assessment of its possible usage during emergency events. Environ Earth Sci 80:176. https://doi.org/10.1007/s12665-021-09497-7

21. Guardia (2018) Geology of the Republic of Panama - Feature Layer. Retrieved 15 November 2019,from:https://www.arcgis.com/apps/mapviewer/index.html?layers=343419d1aca4452585e47eb7f4d012de
22. Gutiérrez E (2021) Informe petrográfico de la roca del acuífero de la Extensión UTP Tocumen, para la Lic. Ana González, pp 1–2
23. Healy R, Cook P (2002) Using groundwater level to estimate recharge. Hydrogeology Journal (2002) 10:91–109, https://doi.org/10.1007/s10040-001-0178-0
24. Ho C, Mojica A, Pinzón R, Díaz I, Llubes M, Pastor L (2017) Non-Invasive Time-Lapse Imaging of Rainfall Infiltration Levels in the Sedimentary Soils of Central Panama. Sustainability in Environment (2017) Vol. 2, No. 2, DOI: https://doi.org/10.22158/se.v2n2p148
25. Jordanova D, Goddu S, Kotsev T, Jordanova N (2013) Industrial contamination of alluvial soils near Fe-Pb mining site revealed by magnetic and geochemical studies. Geoderma 192:237–248. https://doi.org/10.1016/j.geoderma.2012.07.004
26. Kiamco C, Alfaro C, Asensio E, Berman G, Calvo A, DePuy M, Franco O, Franceschi P, Guerra F, García L, Hassel A, Isaac M, Ng E, Ramírez O, Ulloa D, Yinh J (2004) Reglamento de Diseño Estructural para la República de Panamá-2004, pp 1-267
27. Kruseman G, De Ridder N, Verweij J (1970) Analysis and evaluation of pumping test data. The Netherlands: International institute for land reclamation improvement 11:1–200
28. La Estrella de Panamá, P (2012) Vuelven las dudas por la planta de Chilibre. La Estrella de Panamá. Retrieved 15 November 2019, from: https://www.laestrella.com.pa/nacional/121130/dudas-planta-vuelven-chilibre
29. Martinez J, Raiber M, Cendon D (2017) Using 3D geological modelling and geochemical mixing models to characterise alluvial aquifer recharge sources in the upper Condamine River catchment, Queensland, Australia. Sci Total Environ 574:1–18. https://doi.org/10.1016/j.scitotenv.2016.09.029
30. Medici G, West L, Mountney N (2016) Characterizing flow pathways in a sandstone aquifer: Tectonic vs sedimentary heterogeneities. J Contam Hydrol 194:36–58. DOI:10.1016/j.jconhyd.2016.09.008
31. Mojica A (2015) Informe de Tomografía de Resistividad Eléctrica 2 D, Estudio hidrogeológico de las aguas subterráneas del pozo ubicado en el Campus de Investigación de Tocumen UTP, para la tesis de la Lic. Ana González. Panamá, Tocumen: Universidad Tecnológica de Panamá, Centro Experimental de Ingeniería, Laboratorio de Investigación en Ingeniería y Ciencias Aplicada, informe No.: CEI-07-SI-115-2015, pp 1–24
32. Mojica A (2018) Geoelectrical Sounding and Imaging over the Central Zone of Panama. Intech, Chap. 8, pp 137–144, http://dx.doi.org/10.5772/intechopen.74210. Retrieved 12 February 2021 from: http://www.intechopen.com/books/trends-in-telecommunications-technologies/gps-total-electron-content-tec-prediction-at-ionosphere-layer-over-the-equatorial-region%0AInTec

33. Mojica A, Díaz I, Ho C, Ogden F, Pinzón R, Fábrega J, Vega D, Hendrick J (2013) Study of seasonal rainfall infiltration via time-lapse surface electrical resistivity tomography: Case study of Gamboa area, Panama Canal Watershed. Air Soil Water Research 2013:6:131–139. https://doi.org/10.4137/ASWR.S12306
34. Mojica A, Solís J, Ortiz F, Duarte B, Harris J, Pastor L (2012) Detección de aguas subterráneas en los suelos sedimentarios de la Extensión de Investigación de Tocumen de la Universidad Tecnológica de Panamá mediante la imaginería bidimensional de resistividad eléctrica y refracción sísmica durante la época seca. I + D Tecnológico, 8(2), 5–14, *ISSN: 1680–8894*
35. Mustafa Y, Al-Hashemi H, Bukhary A (2017) Characterisation and Index Properties Correlations for Marlstone and Marly Limestone of Saudi Arabia. 2nd World Congress on Civil, Structural, and Environmental Engineering (CSEE'17), Paper No. ICGRE 104, ISSN: 2371–5294, DOI:10.11159/icgre17.104
36. Oke S, Vermeulen D, Gomo M (2017) Intrinsic vulnerability assessment of shallow aquifers of the sedimentary basin of southwestern Nigeria. Jamba Journal of Disaster Risk Studies 10(1):a333. https://doi.org/10.4102/jamba.v10i1.333
37. Servicio de Información Meteorológica Mundial (2008) Retrieved 10th March 2021 from: http://wwis.inm.es/076/c01221.htm
38. Skinner S, Halstead R (1958) Note on rapid method for determination of carbonates in soils. Can J Soil Sci 38(2):189–190
39. Shaqour F, Jarrar G, Hencher S, Kuisi M (2008) Geotechnical and mineralogical characteristics of marl deposits in Jordan. Environ Geol 55:1777–1783. https://doi.org/10.1007/s00254-007-1128-5
40. Shomar B (2015) Geochemistry of soil and groundwater in arid regions: Qatar as a case study. Groundwater for Sustainable Development 1:33–40. https://doi.org/10.1016/j.gsd.2015.12.005
41. Tan H, Liu Z, Rao W, Wei H, Zhang Y, Jin B (2017) Stable isotopes of soil water: Implications for soil water and shallow groundwater recharge in hill and gully regions of the Loess Plateau, China. Agriculture Ecosystems Environment 243:1–9. https://doi.org/10.1016/j.agee.2017.04.001
42. The Constructor (2018) What is RQD (Rock Quality Designation)? Retrieved March 2021 from: https://theconstructor.org/geotechnical/rqd-rock-quality-designation-calculation/20536/
43. Vázquez A, Bautista N (1993) Guía para interpretar el análisis químico de suelo y agua. Departamento de Suelos, Universidad Autónoma de Chapingo, México, N° folleto 1049, pp 1–29
44. Vega D (2004) Informe de Prueba de Bombeo, Pozo de Extensión Tocumen, Centro de Investigaciones Hidráulicas, pp 1–10
45. Weaver R, Syers J, Jackson M (1991) Análisis Químico de Suelos. Ed. Omega (Madrid), ISBN: 978-8428201438. 267 pp
46. Wersin P, Mazurek M, Mäder U, Gimmi T, Rufer D, Lerouge C, Traber D (2016) Constraining porewater chemistry in a 250 m thick argillaceous rock sequence. Chemical Geology 434 (2016) 43–61, doi: 10.1016/j.chemgeo.2016.04.006

47. Zhang X, Hu B, Wang P, Chen J, Yang L, Xiao K, Zhang X (2018) Hydrogeochemical Evolution and Heavy Metal Contamination in Groundwater of a Reclaimed Land on Zhoushan Island. *Water* 2018 10(3):316. https://doi.org/10.3390/w10030316

Figures

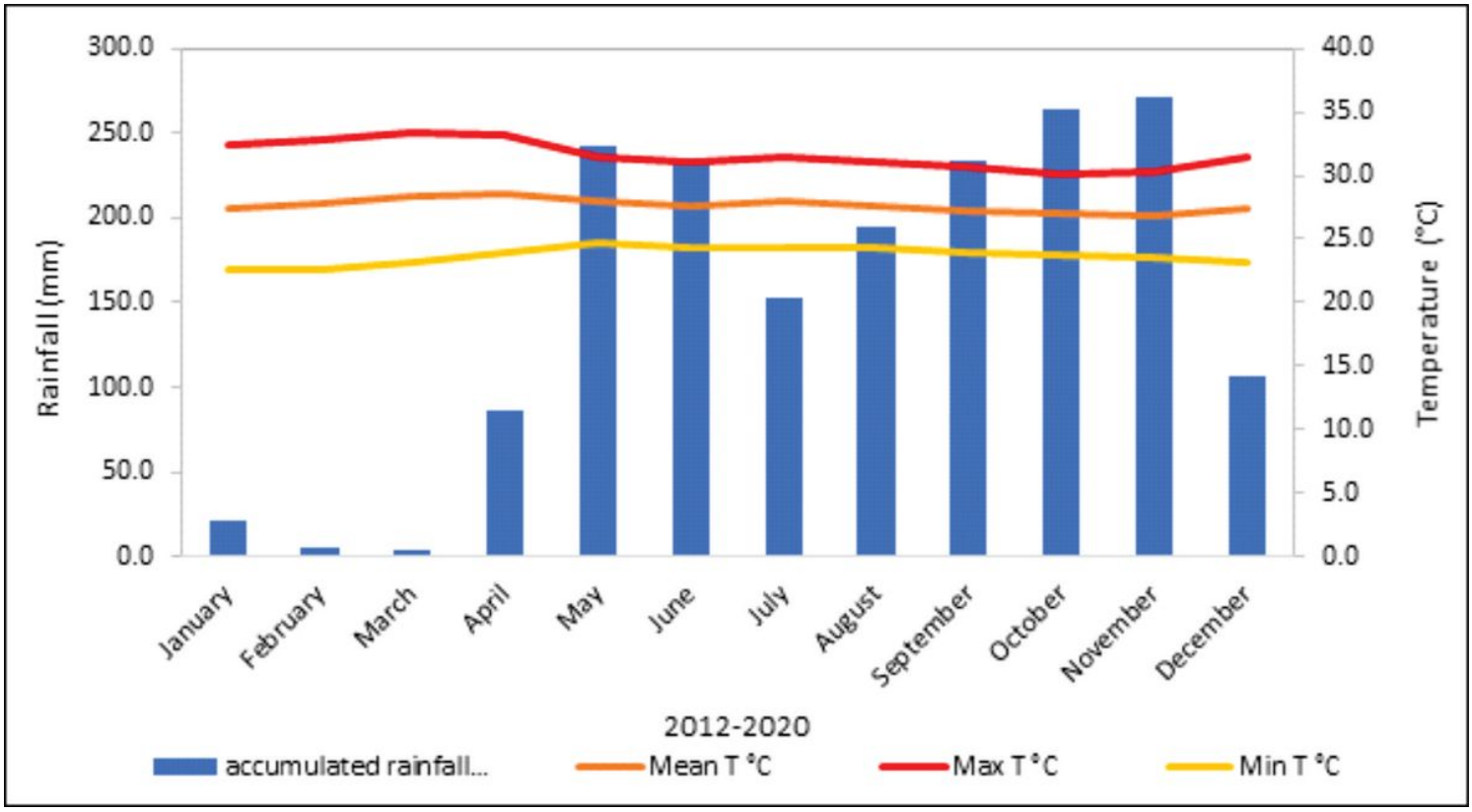

Figure 1

Climograph: Tocumen weather station 2012–2020

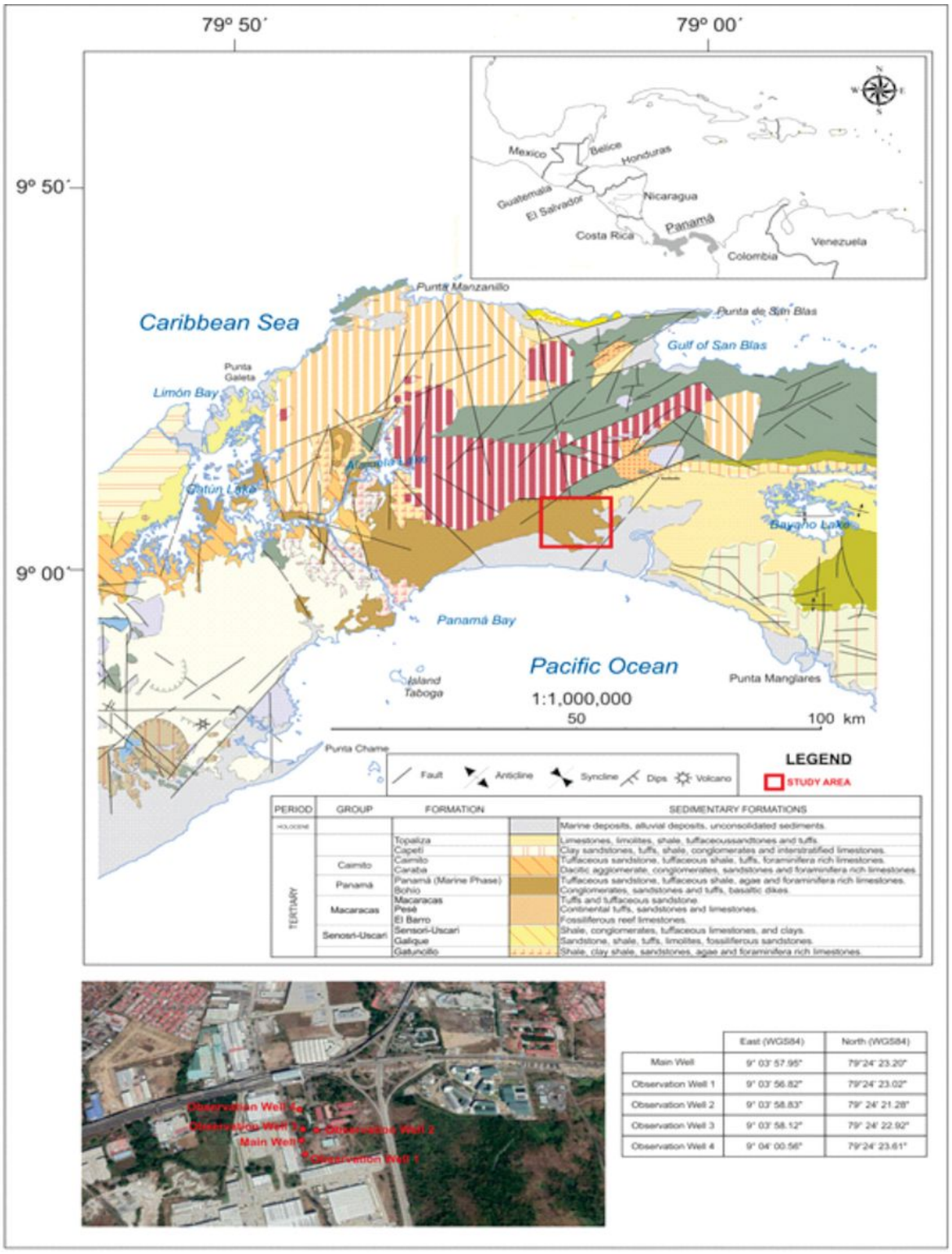

Figure 2

Geological map of the study area (adapted from Guardia 2018). Note: The designations employed and the presentation of the material on this map do not imply the expression of any opinion whatsoever on the part of Research Square concerning the legal status of any country, territory, city or area or of its authorities, or concerning the delimitation of its frontiers or boundaries. This map has been provided by the authors.

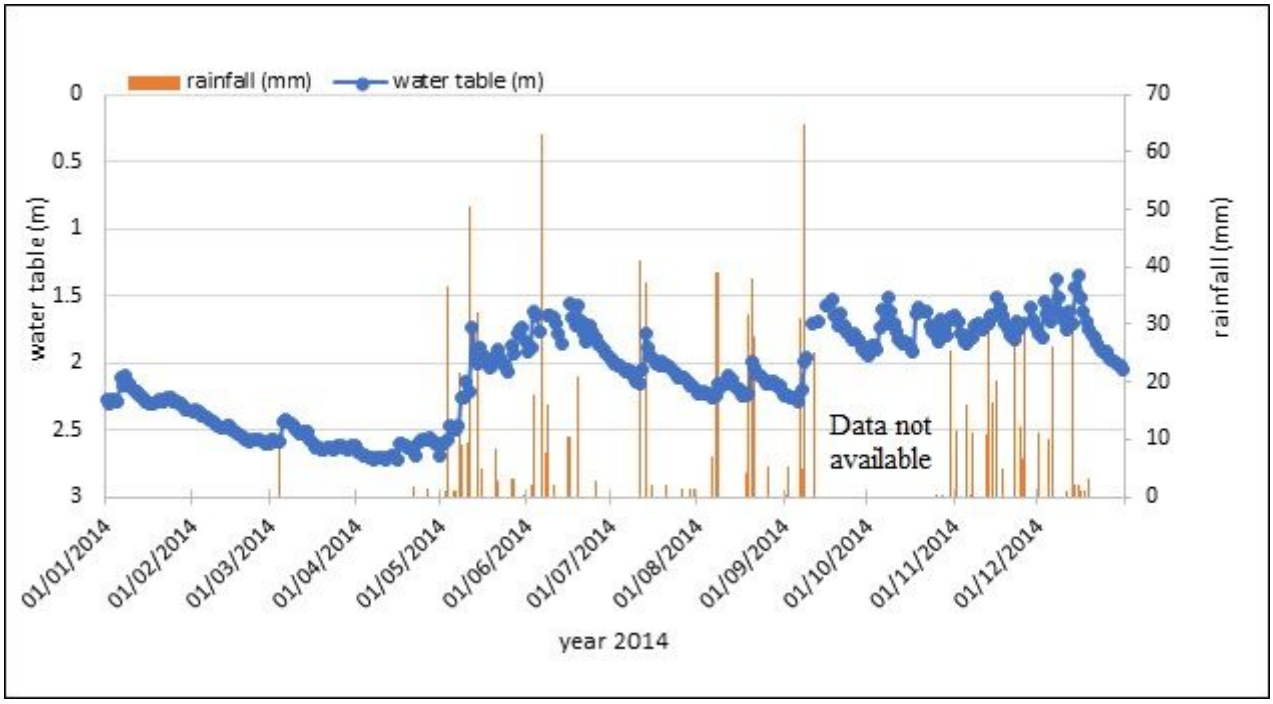

Figure 3

Temporal evolution of the water table vs. rainfall 2014.

Figure 4

Study area: a) Drilling of the well; b) Drill hole profile.

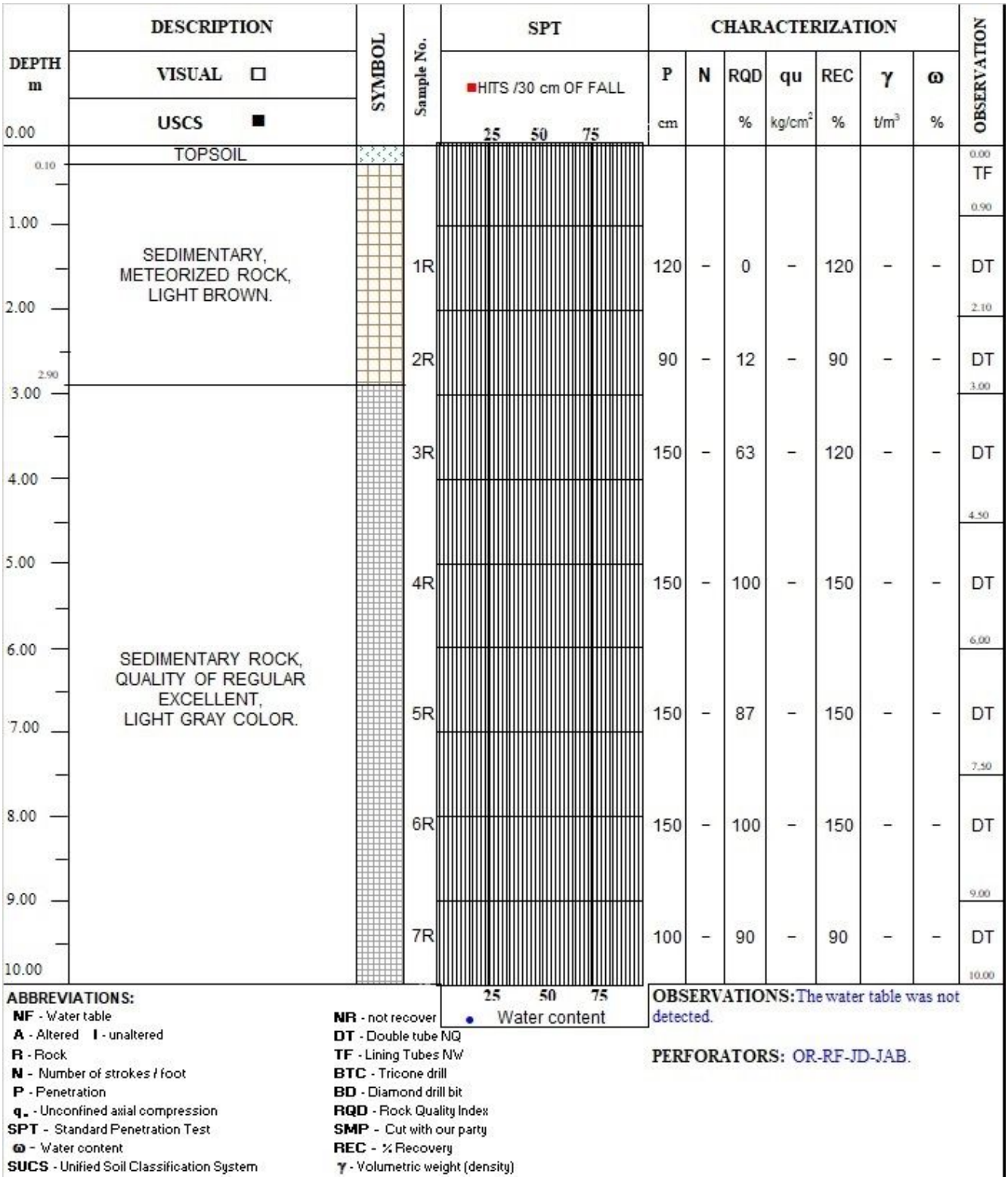

Figure 5

Drilling profile of the drill hole.

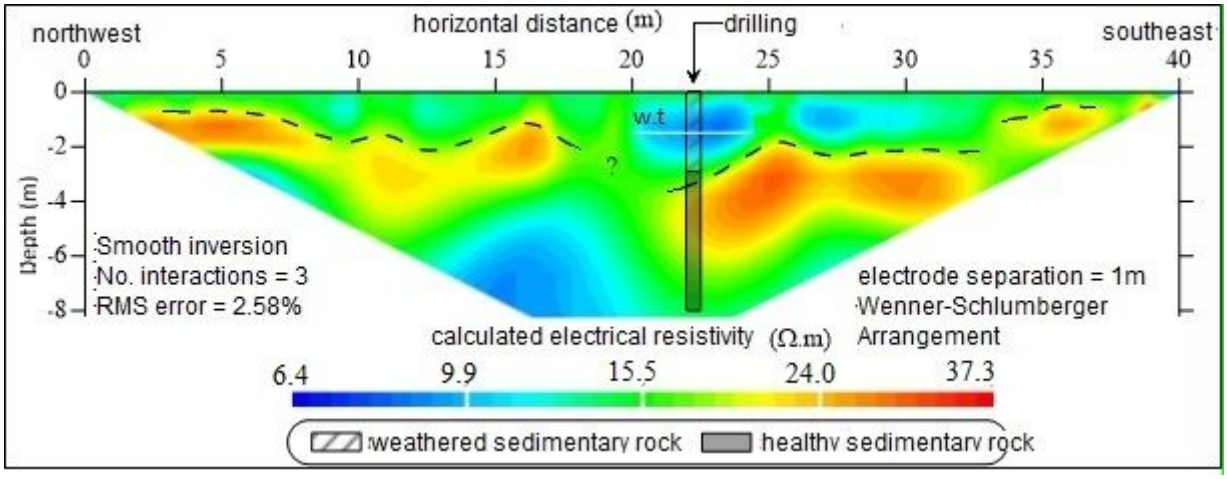

Figure 6

Electrical resistivity tomography obtained using soft inversion as a restriction of the least square optimization method. w.t: water table.

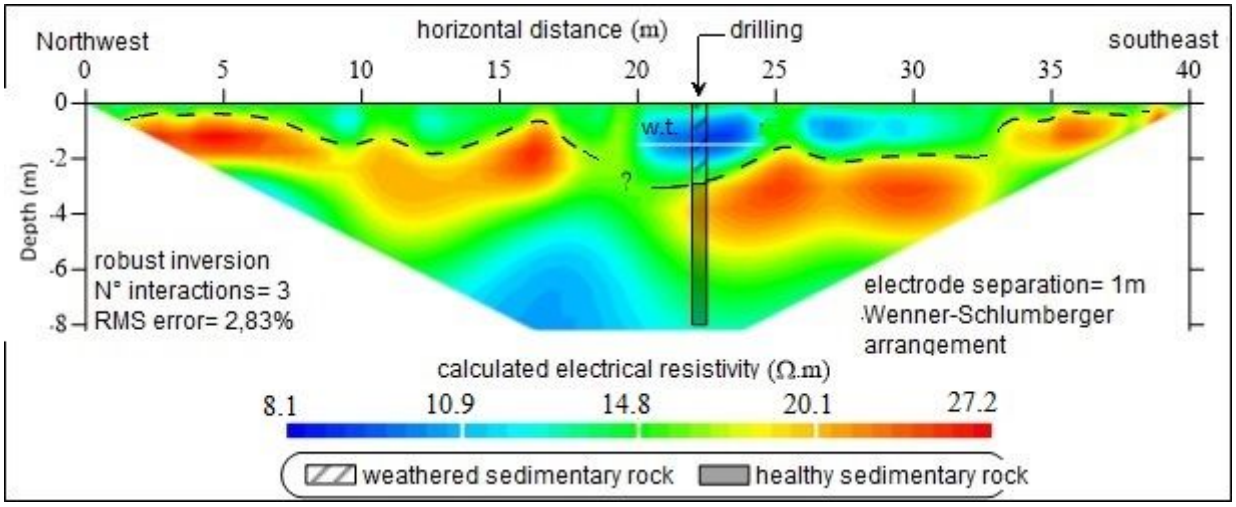

Figure 7

Electrical resistivity tomography obtained by using robust inversion as a restriction of the least squares optimization method. w.t: water table.

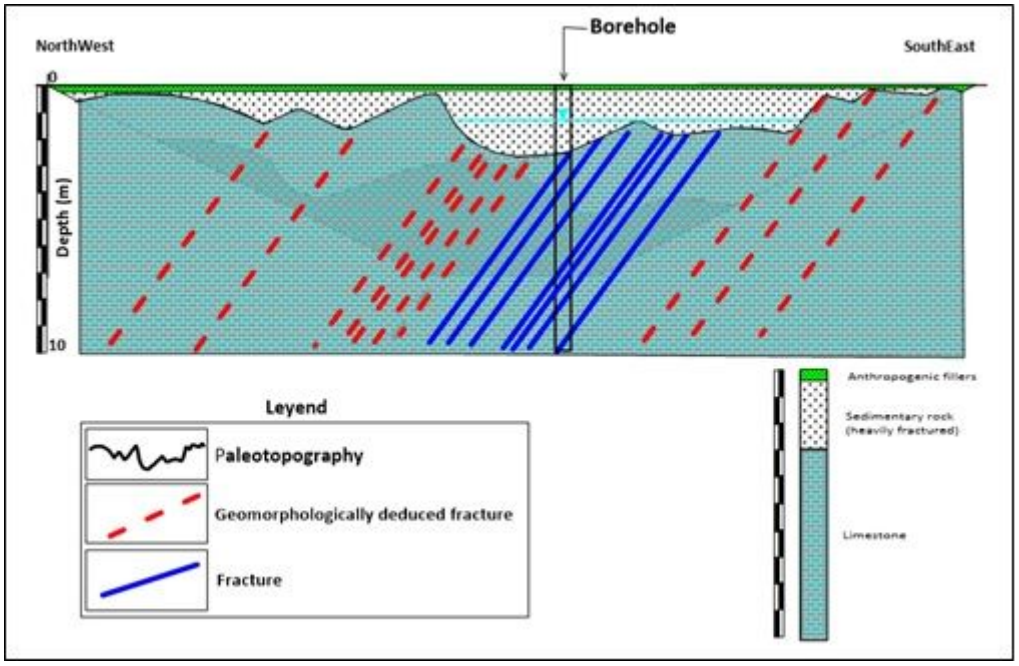

Figure 8

Electrical tomography profile (top image). Geological profile interpreted based on the lithology and fracturing of the borehole (bottom image).

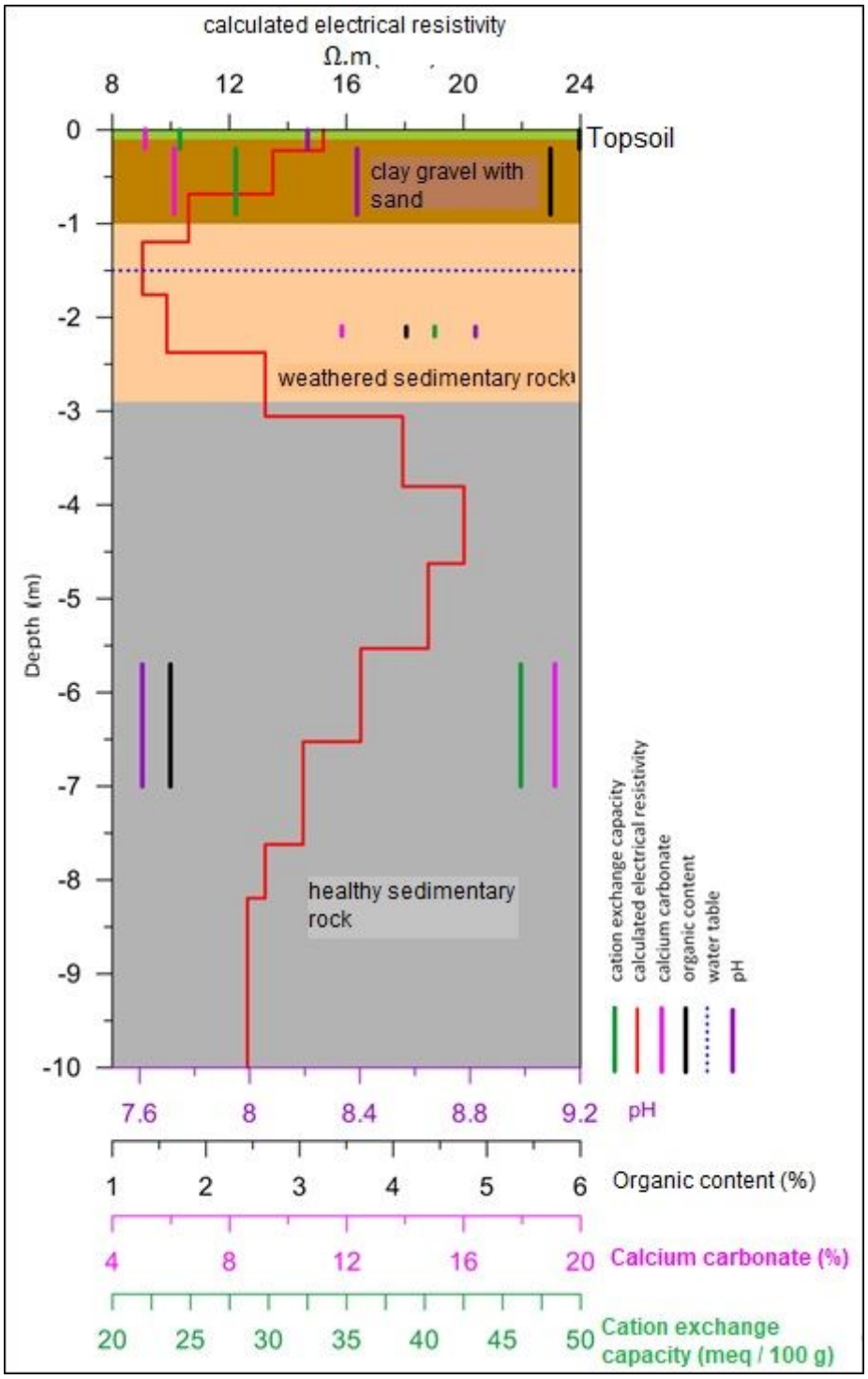

Figure 9

Graphical representation of the stratigraphy of the profile, including values for the geochemistry, and electrical resistivity parameters determined.